RUSSIAN ACADEMY OF SCIENCES

NATIONAL GEOPHYSICAL COMMITTEE

РОССИЙСКАЯ АКАДЕМИЯ НАУК

НАЦИОНАЛЬНЫЙ ГЕОФИЗИЧЕСКИЙ КОМИТЕТ

NATIONAL REPORT

for the

International Association of Geomagnetism and Aeronomy

of the

International Union of Geodesy and Geophysics

2007–2010

НАЦИОНАЛЬНЫЙ ОТЧЕТ

Международной ассоциации геомагнетизма и аэрономии

Международного

геодезического и геофизического союза

2007–2010

Москва 2011 Moscow

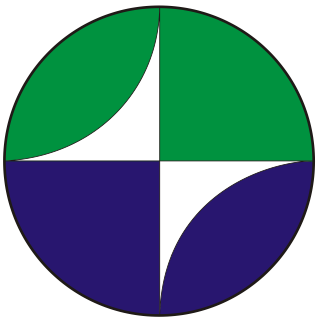

Presented to the XXV General Assembly
of the
International Union of Geodesy and Geophysics

К XXV Генеральной ассамблее
Международного геодезического и геофизического
союза

RUSSIAN ACADEMY OF SCIENCES

National Geophysical Committee

NATIONAL REPORT

for the

International Association of Geomagnetism and Aeronomy

of the

International Union of Geodesy and Geophysics

2007–2010

Presented to the XXV General Assembly

of the

IUGG

2011

Moscow

The Report is prepared by the Section of Geomagnetism and Aeronomy of the National Geophysical Committee of Russia to the XXV IAGA/IUGG General Assembly. Some main results of 2007-2010 are presented on the following topics: 1) Internal Earth's magnetic field; 2) Aeronomic Phenomena; 3) Magnetosphere; 4) Solar wind and interplanetary magnetic field; 5) Observations, instruments, surveys and analysis.

Отчет, подготовленный Секцией геомагнетизма и аэрономии Национального геофизического комитета России к XXV Генеральной ассамблее МАГА/МГГС, отражает некоторые основные результаты исследований, выполненных российскими учеными в 2007 – 2010 гг. по следующим разделам: 1) внутреннее магнитное поле Земли; 2) аэрономия; 3) магнитосфера; 4) солнечный ветер и межпланетное магнитное поле; 5) приборы, обсерватории, службы и анализ данных.

Contents

Foreword

This report containing a review of the activities and scientific researches in 2007-2010 in Russia has been compiled for the presentation to the International Association of Geomagnetism and Aeronomy at the XXV General Assembly of IUGG.

There are five sections in the report according to the IAGA Divisions I-V. The preparation of this report has been organized by the National Commission on the Geomagnetism and Aeronomy and the National Geophysical Committee as a collective effort of the team of authors. Only minimal editorial work has been done when putting all these parts together, preserving, thus the diversity in styles and approaches.

The report cannot be considered as comprehensive review of the principal achievements during this period of time in this field of science in Russia. Moreover, some arbitrariness in the choice of the material makes the report far from being complete. Many important results are not mentioned at all. Bearing in mind all these restrictive circumstances we hope that the readers who are interested in this field of science can find useful sources of information in this report.

The Editors

I. Internal Earth's Magnetic Fields

Earth's Magnetic Field Atlas

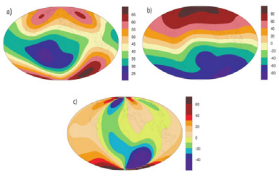

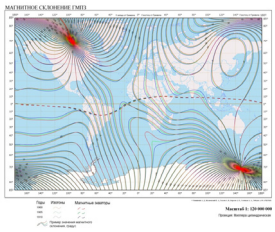

The Geophysical Center of the Russian Acacadmy of Sciences and IZMIRAN have completed preparation of the electronic version of the Atlas of the Earth's magnetic field (EMF). The Atlas is a unified set of physical, general geographic, thematic and historical maps of EMF, as well as background (text and spreadsheet) materials to thoroughly study the versatile EMF from 1500 up to now. The Atlas is designed not only to scholars and specialists in the field of EMF, but also for a wide range of customers from adjacent academic and applied areas, and readers interested in this problem. This is a world first attempt to create such Atlas and it represents a fundamental mapping product with the most complete scientific characteristics of EMF. It is further assumed edition of the Atlas in printed form.

- Contact E. Jalkovsky (e.jalkovsky@gcras.ru)

The study of electromagnetic and telluric anomalies of Baikal rift zone (BRZ)

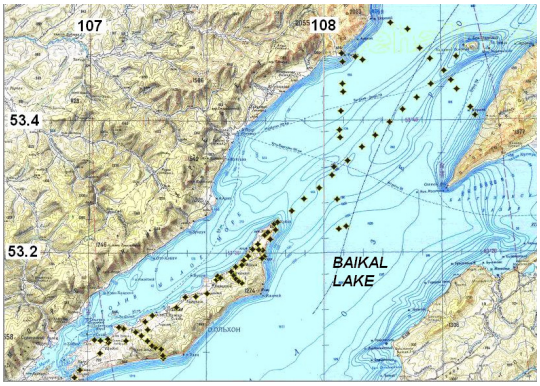

From March 2009 to July 2010, electromagnetic anomalies in the water area of Lake Baikal were examined.

Field measurements were carried out on ice of Lake Baikal in March 2009. The measurements were made along and across the Academichesky mountain range axis.

The expeditionary measurements were performed on Olkhon in July 2010. Field measurements of the magnetic-field total vector (DIF-measurements) were conducted at 21 points. The measurements of the module of the full vector (F-measurements) were made at 49 points. The special magnetic high-density survey (F-measurements) was organized on Olkhon (a step of 100 m) at 83 points. The observations revealed magnetic anomalies in the measurement region. There are unique particularities in F distribution along special profiles on Olkhon as well as two strong anomalies of the field with the amplitude over 200 nT. The linear extension of these anomalies is about 0.5 km.

A difference was found between magnetic declinations D in the BRZ region (Olkhon, Uzury observatory) and Irkutsk (Patrony observatory) from March 2009 to July 2010. A decrease in the declination at Uzury observatory is 3 arcmin; at Patrony observatory, 7.5 arcmin.

www.iszf.irk.ru

Contact R. Rakhmatulin rav@iszf.irk.ru

The first calculation of the South magnetic pole position

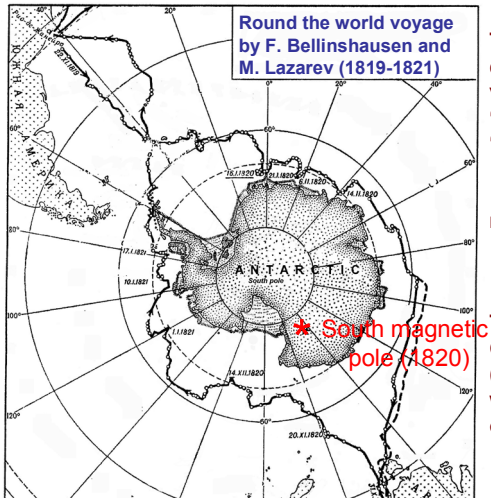

The route of voyage of "Vostok" and "Mirny" marked by magnetic measurement sites (circles).

The material of measurements of magnetic declination during Antarctic round the world voyage (1819-1821) of Russian ships "Vostok" (captain F.F. Bellinshausen and "Mirny" (captain M.P. Lazarev) was analysed. We presented the map with the ship route and location of sites where the magnetic measurements were performed. On the base of these data F.F. Bellinshausen was the first who calculated the magnetic South pole position (76^{O} S, 142.5^{O} E). This calculation was performed before Gauss (72^{O}35' S, 152^{O}30' E) and Ross (75^{O}05' S, 154^{O}08' E). Calculation by Ross was performed on the base of data which obtained 20 years later than Bellinshausen data.

Contact O.M. Raspopov (SPbF IZMIRAN) :

oleg@or6074.spb.edu

Balloon Gradient Measurements of Total Magnetic Field

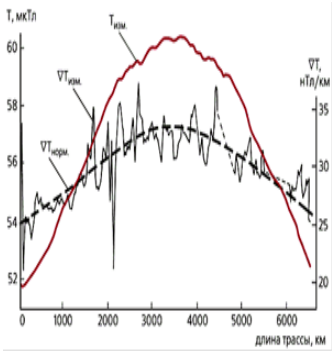

A new technique for processing balloon gradient magnetic data has been developed in order to reliably derive crustal magnetic field from balloon magnetic data, create comprehensive lithospheric magnetic models as well as estimate the accuracy of world magnetic models such as IGRF and WMM.

To achieve these goals at the compiled gradient magnetic profile we identified the areas where prominent magnetic anomalies have not been observed. Abscissas of identified locations have been defined and transferred to the magnetic profile, from which the main and external fields have been removed. Ordinates for these locations defined the accuracy of main magnetic field model. This approach can be implemented for correction of identified magnetic anomalies and analysis of accuracy of world magnetic models. The method has fundamental value and allows to study at basic level a phenomenon of abnormal magnetic field

Contact: tsvetkov@izmiran.ru

II. Aeronomic Phenomena

Dynamics of ionospheric and atmospheric characteristics during strong stratospheric warmings

Experiment conditions:

- North-West region of Russia in Jan. – Feb. 2008, magnetically quiet period.
- Complex experiment data including radiophysical and optical instruments: radar, ionosondes, GPS receivers, zenith photometers.
- High time resolution - ~ 1 min.
- **The stratospheric temperature exceeded its average level by 70 deg**.

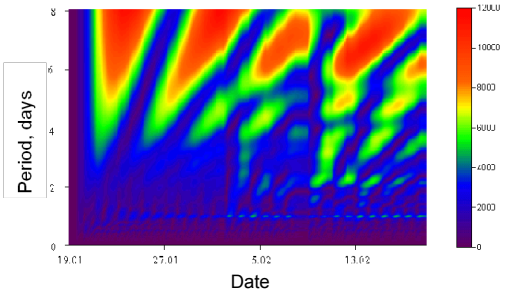

Amplitudes of f0 F2 variations above Irkutsk during stratospheric warmings.

Spectral analysis of time variations of ionospheric parameters reveals
(1) maximum amplitude of planetary scale wave-like disturbances of electron density in the F-region with a period of 5 – 8 days,
(2) large scale drifting disturbances with a period of 1 - 4 hours.

Contact V.I. Kurkin (kurkin@iszf.irk.ru)

Anomalous high values of 557.7 nm mid-latitude airglow intensity during periods of winter sudden stratospheric warmings in Eastern Siberian region

Anomalous high values of 557.7 nm airglow intensity can be caused by high level of mean intensity of this emission in winter months in the period of high solar activity. During sudden stratospheric warmings (SSW), variations with the periods about several days superpose on the mean level of 557.7 nm airglow intensity, providing anomalous high diurnal values of this airglow at the peaks. High airglow intensity in winter months in Eastern Siberia may be connected with 2-3 times increasing of atomic oxygen density at the emitting heights of 85-115 km during periods of high solar activity. The received results are in good agreement with the atomic oxygen density variations measured at high latitudes in Eastern Siberia (Yakutsk) during the 23-rd solar cycle.

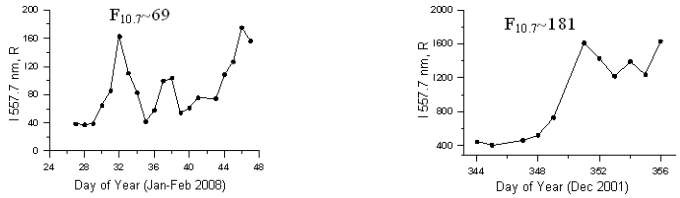

Diurnal variations of 557.7 airglow during SSW periods at 2 levels of solar activity. Annual values of F10.7 index are specified.

Contact V.I. Kurkin (kurkin@iszf.irk.ru)

Regional empirical model of ionospheric plasma density

A regional empirical model of ionospheric plasma density has been created on the basis of longterm measurements by the unique radiophysical tools of the ISTP SB RAS (incoherent scatter radar, digital ionosondes). The model allows improving the International Reference Ionosphere (IRI model) prediction because of taking into account the regional peculiarities. The diurnal-seasonal pattern of the F2 peak density (NmF2, in $10^5 \cdot cm^{-3}$) under low solar activity (a,b) and the rate of NmF2 increase (in $10^5 \cdot cm^{-3}/100$ sfu) with the solar activity (c,d) given by the regional model (a,c) and IRI (b,d) for the midlatitude ionosphere are shown in the Figure.

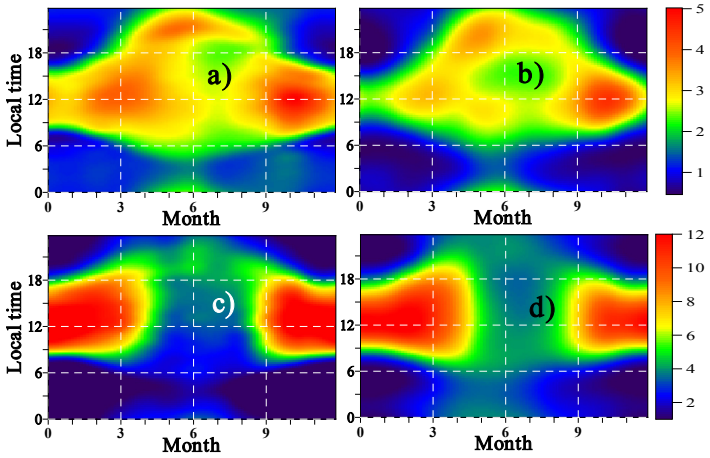

Contact
K.G. Ratovsky
(ratovsky@iszf.irk.ru)

Results of ionospheric activity analysis

The automated method for studying the ionospheric activity level has been developed on the basis of long-term measurements by the unique radiophysical tools of ISTP SB RAS . The complete analysis of the electron density disturbances has been carried out. The developed method of analysis of long-term experimental data sets provides a possibility to automate the process for revealing statistical and morphological regularities of ionospheric disturbances.

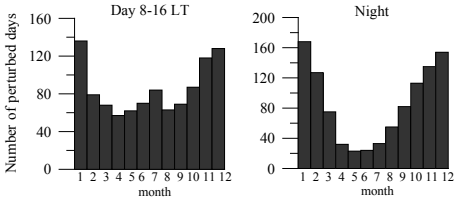

Seasonal pattern of total ionospheric activity

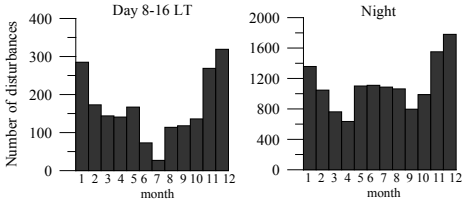

Seasonal pattern of wavelike ionospheric activity

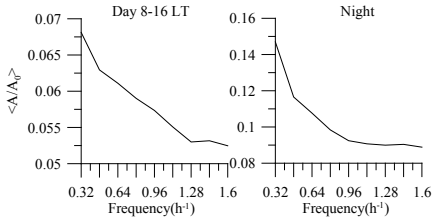

Frequency dependence of disturbances amplitude

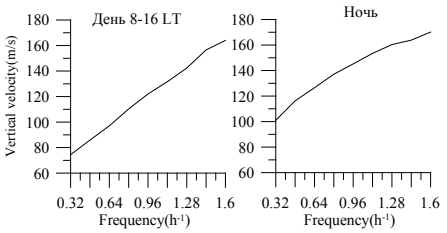

Frequency dependence of vertical velocity

Contact A.V. Medvedev (medvedev@iszf.irk.ru)

3D Numerical simulations of ozone response to geomagnetic storms

The response of atmospheric chemical composition in both polar regions was studied with CAO-3D photochemical-transport model for the middle atmosphere (*Krivolutsky et al., 2006)*. Relativistic electrons precipitating from radiation belts during geomagnetic storms and solar protons can penetrate below 100 km into the polar atmosphere sometimes reaching the stratospheric levels loosing energy and causing strong ionization (each 35 eV gives one pair of ions). This leads to additional production chemical compounds which destroy ozone by chemical catalytic cycles.

Photochemical simulations for geomagnetic storms in October - November 2003 show strong ozone depletion over both polar region. Nevertheless, Northern and Southern polar regions response differently mostly due to two factors: polar cap expansion during the geomagnetic storm and the effect of horizontal transport. The results of photochemical simulations generally agree with satellite observations.

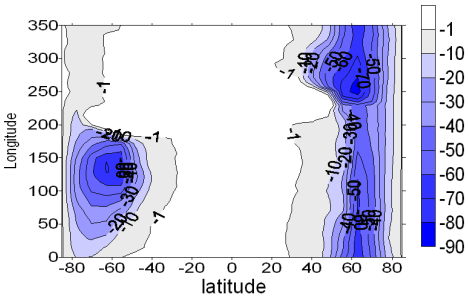

Global ozone response (%) at 66 km height to energetic particle fluxes as simulated with 3D photochemical model for 28 October 2003.

Contact A.A. Krivolutsky
(alexei.krivolutsky@rambler.ru)

Long-term variations of LF-VLF signals

3-year monitoring of LF – VLF signals from radio stations in the mid-latitude ionosphere located at distances up to 2000 km from the receiver (Michnevo, 54.94°N, 37.73°E) showed that during quiet Sun in the absence of geomagnetic disturbances, the signals varied significantly. This evidences that on the ways of signal propagation, the ionospheric D and E layers are modified by litosphere-atmosphere disturbances.

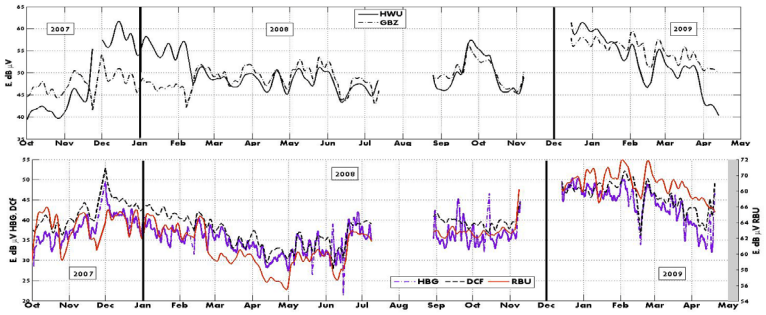

Radio Station	Coordinate	Distance from Michnevo, km	Frequency, kHz	Power, kW
HWU	46.64N; 1.05E	2702	18.3	200
GBZ	52,72N; 3.06E	2650	19.6	30
RBU	55.73N; 38.2E	93	66.6	10
HBG	46.40N; 6.26E	2387	75	20
DCF-77	50.0N, 9.0E	2006	77.5	50

Contact Yu.I. Zetzer
(zetzer@idg.chph.ras.ru)

Empirical model of auroral precipitation power during substorms

An energetic model of auroral precipitation during substorms was developed basing on statistical study of electron precipitation features observed by the DMSP F6 and F7 spacecraft. Auroral boundary positions (Fig. 1) and the average values of electron precipitation flux during all substorm phases were used to calculate the precipitation power (UA).

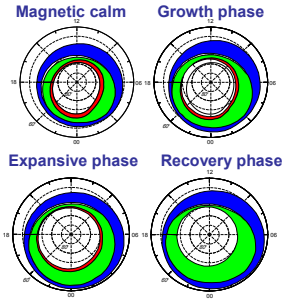

Fig. 1. Global distribution of auroral precipitation

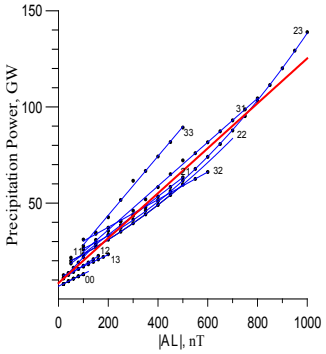

The model enables to obtain the average precipitation power during all substorm phases for any AL index intensity.

Fig. 2. Precipitation power during all substorm phases versus AL Index intensity

At the final stage of substorm expansive phase the global precipitation power increases from about 30 GW for the substorm of |AL|=150 nT to 140 GW for the substorm of AL|=1000 nT. A simple linear relation UA(GW)=8.4-0.12·AL(nT) was deduced (Fig .2).

Contact V.G. Vorobjev (vorobjev@pgia.ru)

The effect of liquid-propellant rocket engines (LPRE) of the cargo transportation vehicle (CTV) "Progress" on the surrounding ionosphere.

Space experiments "Plasma-Progress" (September 2007, February and September 2008, February and September 2009) involved measurements of parameters (reflecting characteristics, sizes, density, etc.) of large-scale plasma formations produced by LPRE functioning onboard CTV "Progress" with different directions of exhausting plumes relative to the CTV motion.
With the use of the ISTP SB RAS Incoherent Scatter Radar, it is revealed that in the surrounding ionosphere, a low electron density area (20–40% less than the background value, lifetime is 10–15 min) is formed after a short thruster firing (5 sec).

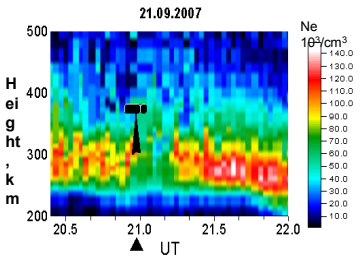

Dynamics of the formation of low electron density area after the thruster firing (▲). Position of the cargo transportation vehicle and thruster plume is shown.

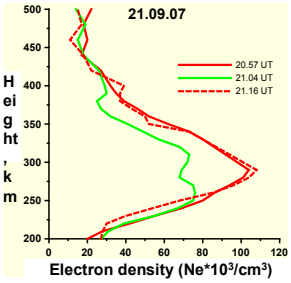

Electron concentration profiles: the background (—), disturbed (—) and recovered (- -) ionosphere.

Contact A.V. Medvedev (medvedev@iszf.irk.ru)

Ionospheric response to solar eclipse on 1 Aug. 2008 observed by radio wave back-scattering due to natural ionospheric disturbances (partial reflections) and artificial periodic irregularities (API).

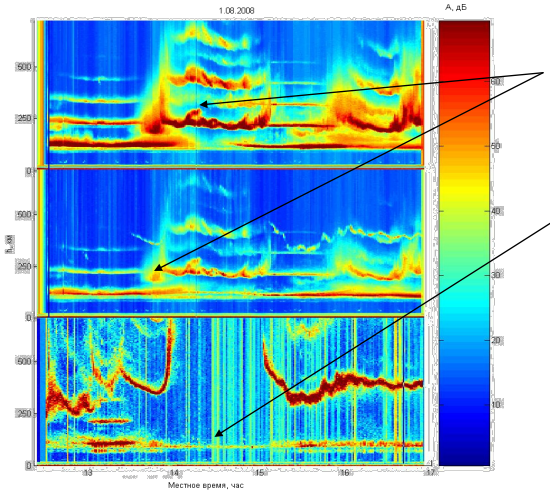

During the solar eclipse (1 August 2008: start 13:07; max 14:16; end 15:22) partial reflections change, radio emission of 4.7 MHz is no longer reflects from the ionosphere and the API disappeared.
Measurements of partial reflections were used to determine the **electron density** in the ionospheric D-layer, which **decrease significantly during the eclipse**.

Contact V.L. Frolov
(frolov.418@nirfi.sci-nnov.ru)

III. Magnetospheric Phenomena

Non-adiabatic particle acceleration in the magnetotail current sheet (1).

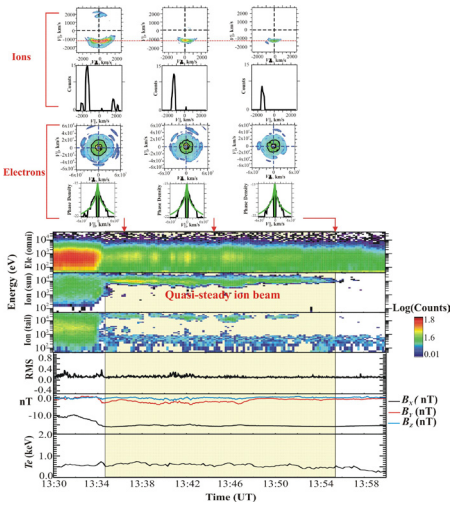

Fig. 1. An example of Geotail observation of quasi-steady ion beam non-adiabatically accelerated in the CS at closed magnetic field lines.

Particle acceleration in the magnetotail Current Sheet (CS) usually was related with a magnetic reconnection. Analysis of ion and electron velocity distribution functions registered in 1000 crossings of Plasma Sheet Boundary Layer (PSBL) by Geotail and Cluster spacecraft revealed that during geomagnetically quiet periods non-adiabatic ion acceleration occurs in the CS at closed magnetic field lines with finite positive B_z, i.e. rather far earthward from the reconnection region. Accelerated ions are ejected into the PSBL where they form energy and pitch-angle collimated ion beams streaming towards the Earth. Duration of such beams may exceed 20 min.

Contact E.E. Grigorenko
(elenagrigorenko2003@yahoo.com)

Non-adiabatic particle acceleration in the magnetotail current sheet (2).

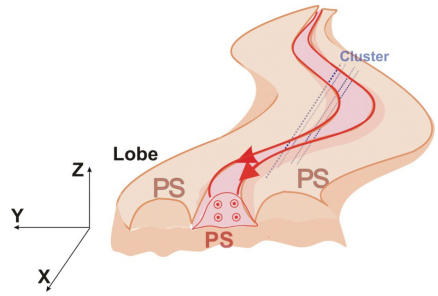

Fig 2. A sketch of spatial structure of high-latitude surface of the PSBL during quiet geomagnetic intervals. The surface is non-uniform and consists of magnetic flux tubes with localized cross-section filled by accelerated field-aligned ion beams (shown by pink color) and of magnetic flux tubes filled by more isotropic PS-like plasma (shown by light-brown color).

The sources of non-adiabatic ion acceleration in the CS (so-called resonances) may be localized in the dawn-dusk direction and between them ions experience strong scattering and heating. As a result, during quiet time intervals the high-latitude surface of the PSBL may be non-uniform and consist of the magnetic flux tubes with strictly localized cross-section ($\leq 0.5 \times 0.5\ R_E$) filled by energy-collimated field-aligned ion beams and of magnetic flux tubes containing more isotropic plasma resemble the plasma of the plasma sheet.

Contact E.E. Grigorenko
(elenagrigorenko2003@yahoo.com)

Tailward and earthward flow onsets observed by Cluster in a thin current sheet.

From a Cluster survey of the magnetotail during 2001–2007, distribution of plasma flow onsets was investigated, basing on 49 episodes of thin current sheet observations ending with plasma sheet activity onsets. The onsets were defined as flow bursts and/or electric current decrease and/or B_z increase after a period of local quietness (in many cases with signatures of growth phase). Such onsets at 17–20 R_E of radial distance were accompanied mainly by tailward flows with negative B_z. At 11–17 R_E, earthward flows dominated, except the premidnight sector, where flows of both directions were observed. Tailward velocities were often rather small, within 200–300 km/s. We interpret such tailward flows as reconnection pulses occurring on the closed field lines in the stretched magnetic configuration. Ten activity onsets were not accompanied by plasma flows (faster than 100 km/s). Preonset current density was larger on average in the premidnight and midnight sector in comparison with the postmidnight.

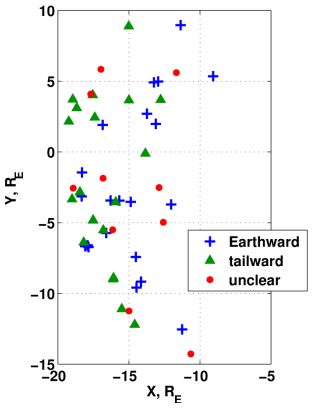

Contact A.A. Petrukovich
(apetruko@iki.rssi.ru)

The Earth's magnetopause and bow shock modeling using Prognoz/Interball observations

- 331 magnetopause and 232 bow shock crossings by Prognoz, Prognoz 2-6, 9 since 1972 to 1983
- 2625 magnetopause and 1150 bow shock crossings by Interball 1 during 1995 and 1999

$$y(x) = \frac{D}{\pi}\arctan\left(\frac{\pi}{D}\sqrt{2R_0(r_0 - x)}\right)$$

(r_0 – subsolar distance, R_0 – nose radius of curvature, b – bluntness of the magnetopause)

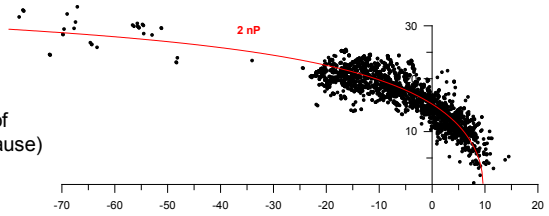

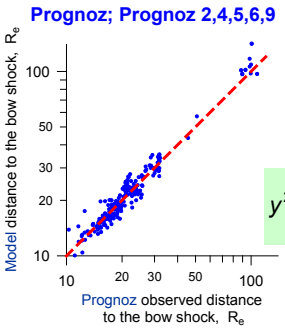

Fitted parameters - magnetopause stand off distance r_0, nose curvature radius R_0 and bluntness b = $-8\pi/3\cdot(\pi R0/D)^2$ - from MP model were used as entry parameters for the bow shock model

$$y^2(x) = 2R_s(r_0 + \Delta - x) + \frac{(r_0 + \Delta - x)^2}{M_s^2 - 1}\left(1 + \frac{b_s M_s^2 - 1}{1 + d_s(r_0 + \Delta - x)/R_s}\right)$$

Contact M.I.Verigin (verigin@iki.rssi.ru)

ULF wave (1-6 mHz) signature of a magnetic storm

Based on the analysis of the observations of the globally distributed ground-based Pc5 range geomagnetic pulsations during several strong magnetic storms, the ULF maps have been constructed in the coordinates (geomagnetic latitude – MLT) for each given UT interval. The typical ULF wave signature of the different storm phases has been established .

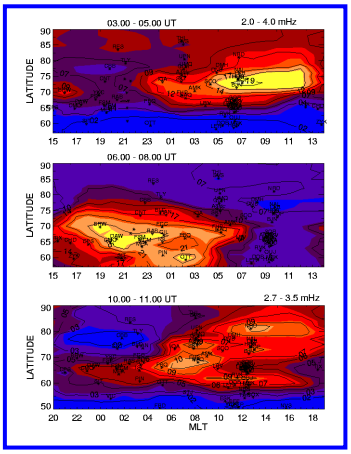

In the storm initial phase, the strongest 1-6 mHz geomagnetic pulsations are observed at the morning sector of the polar (Φ>70) latitudes.

In the storm main phase, the strongest irregular 1-6 mHz Pi3 magnetic pulsations are observed in the night side of the auroral zone, and the largest continues Pc5 pulsations are typical for the morning side of the auroral latitudes.

In the storm recovery phase, the ULF activity shifts to the polar latitudes, and the strongest Pc5 pulsations are recorded at the Φ > 70 mostly in the day time sector.

Contact N.G. Kleimenova

(kleimen@ifz.ru)

Experimental study of inharmonic magnetospheric oscillations

A pronounced difference exists between the theory, which definitely indicates that magnetospheric oscillations are inharmonic, and the experimental study of geomagnetic pulsations.

The Pc5 observations at the IMAGE meridional chain of stations were used to search for nonlinear distortions in latitude profile of the pulsation amplitude. Using a specific event, it has been indicated that the Pc5 amplitude peak shifts northward along the meridian with decreasing oscillation amplitude. The coefficient of nonlinear distortions in the latitude profile is determined. It is shown that geomagnetic pulsation inharmonicity can be entirely studied experimentally.

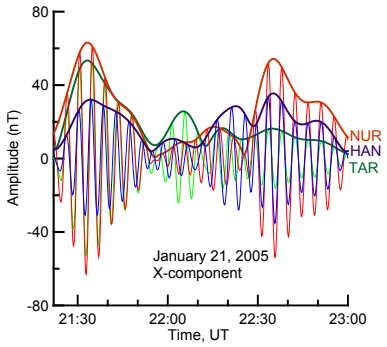

Two wave packets of Pc5 oscillations, registered at three stations of the IMAGE meridional chain. The filtered oscillograms and their envelopes are shown for each station.

Contact A.S. Potapov
(potapov@iszf.irk.ru)

The new ULF-index of geomagnetic pulsation activity

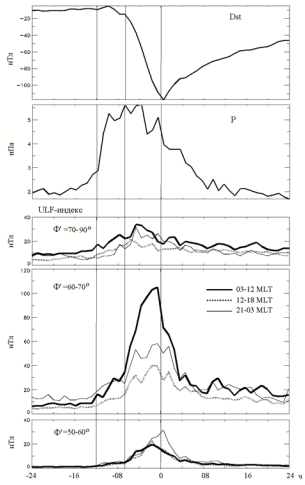

The new ULF-index of the geomagnetic Pc5 (f=1.7-6.0 mHz) pulsation activity has been developed for any given latitude range. The empirical model of the spatial-temporal Pc5 pulsation dynamics has been elaborated applying to the different phases of magnetic storms, caused by the coronal mass ejection (CME). It was found that in the initial storm phase, the strongest ULF wave activity was observed at the morning side of the polar latitudes, probably, due to direct penetration of the solar wind hydromagnetic waves. In the storm main phase, the strongest pulsation activity was not observed at the night sector, as it was commonly expected. The strongest Pc5 range wave amplitude was recorded before the local noon at the auroral zone latitudes demonstrating the typical signature of the field line resonance structure.

Contact O.V. Kozyreva
(kozyreva@ifz.ru)

Dst-index averaged for 19 strong magnetic storms, solar wind dynamic pressure (P), and ULF-index at different latitude zones for 3 intervals of local magnetic time: morning (03-12 MLT), afternoon (12-18 UT), and night-time (21-03 MLT). The vertical fine lines show the border of different storm phases.

Generation of subauroral proton emissions.

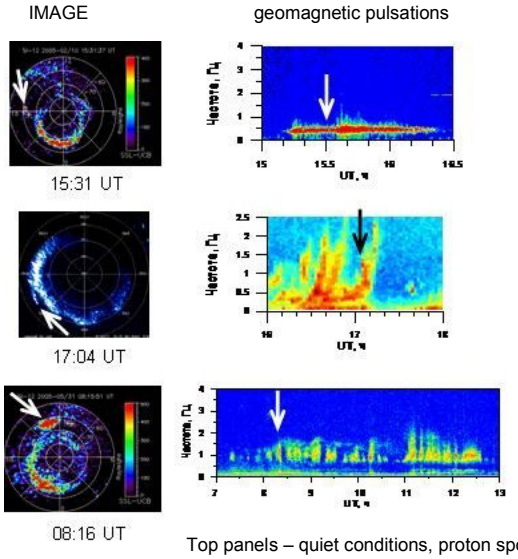

Top panels – quiet conditions, proton spot.
Middle panels – substorm, proton arcs - plasmaspheric tail or plume.
Bottom panels – ram pressure impulses, proton flashes.

Optical measurements on IMAGE were compared with simultaneous ground-based data on geomagnetic pulsations of 0.1-5 Hz. These pulsations are the indicator of electromagnetic ion-cyclotron waves.
It is shown that energetic electron (E>10 keV) precipitations producing proton (Hα) emissions, are caused by cyclotron instability of ring current protons. Space-time features of proton emissions depends on the geometry and evolution of the contact region between cold and hot plasmas in the magnetosphere and also on the solar wind ram pressure.

Contact A.G. Yakhnin
(yahnin@pgia.ru)

Estimating the parameters of the current disruption region in the magnetotail during magnetic disturbances.

Two active phases of a substorm are identified: relatively weak pseudobreakup phase (PSR) originating in the region of closed field lines, and the following expansion phase (TLR) appearing due to reconnection in the “open” magnetotail. The PSR phase usually not ceases but continues during TLR.

Main large scale parameters of the current disruption region are estimated using (1) the distribution of field aligned current density in the ionosphere and (2) two-dimensional thin current sheet approximation in the magnetotail.

Contact V.M. Mishin (mishin@iszf.irk.ru)

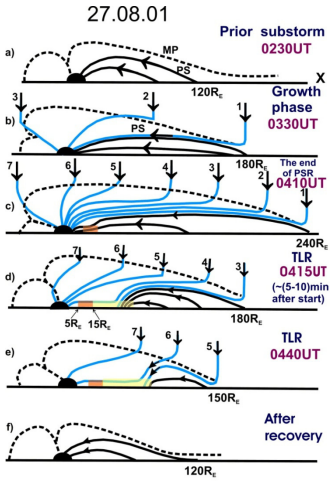

Black – ‘closed’ field lines, **Blue** – ‘open’ field lines, **Red** – PSR close to the Earth, **Yellow** - PSR/TLR

Eigenmodes of thin anisotropic current sheet and their influence on the initiation of geomagnetic disturbances.

Stability of the collisionless current sheet relative to eigenmodes which may propagate in a fan-like manner obliquely to the magnetotail axis was analyzed theoretically. The model takes into account pressure anisotropy and small normal magnetic field Bz, existing in the tail. It is found that for any angle of perturbation propagation, the increasing rate of oblique waves is positive for real parameters of the magnetotail due to an excess of free energy in the anisotropic current sheet.
The theory predicts that in the magnetospheric current sheet, a fan of oblique wave modes can be generated, which have properties of both kink and tearing waves.

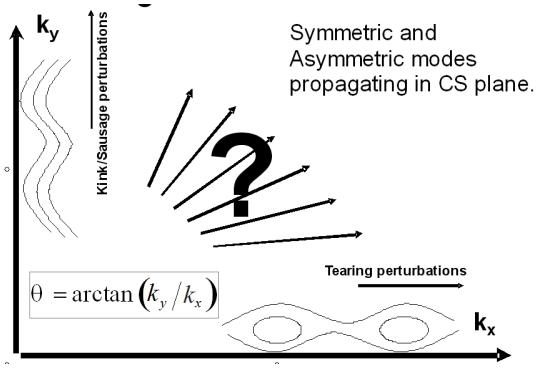

Contact A.V. Artemiev
(ante0226@yandex.ru)

Generation of subauroral proton emissions.

IMAGE

geomagnetic pulsations

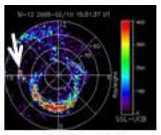

15:31 UT

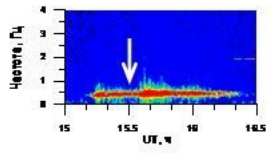

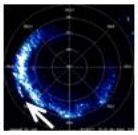

17:04 UT

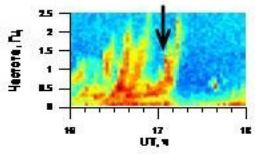

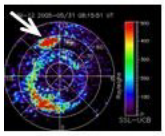

08:16 UT

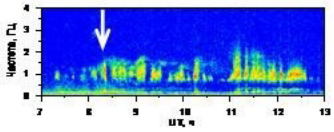

Top panels – quiet conditions, proton spot.
Middle panels – substorm, proton arcs - plasmaspheric tail or plume.
Bottom panels – ram pressure impulses, proton flashes.

Optical measurements on IMAGE were compared with simultaneous ground-based data on geomagnetic pulsations of 0.1-5 Hz. These pulsations are the indicator of electromagnetic ion-cyclotron waves.
It is shown that energetic electron (E>10 keV) precipitations producing proton (Hα) emissions, are caused by cyclotron instability of ring current protons. Space-time features of proton emissions depends on the geometry and evolution of the contact region between cold and hot plasmas in the magnetosphere and also on the solar wind ram pressure.

Contact A.G. Yakhnin
(yahnin@pgia.ru)

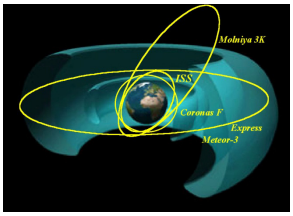

Data bases on radiation conditions in the near-Earth's space

http://smdc.sinp.msu.ru

Space Monitoring Data Center of SINP MSU (SMDC) collects the data of space experiments (CORONAS-F, METEOR-3M, ISS, Universitetsky-Tatyana etc.) as well as scientific and applied models for studying the geomagnetic and radiation conditions in the near-Earth's space environment. SMDC MSU provides access to databases of past and real-time data measured during MSU's space experiments on-board Russian satellites. Web-based services allow integration of data with the models of geomagnetic fields and space radiation. They provide the radiation monitoring and control of the space environment on the basis of near-real-time measurements.

A satellite Universitetsky-Tatyana is the first Education project of Lomonosov Moscow State University. Its main purpose is scientific and educational activity on the basis of experimental data obtained from the small spacecraft.

Latest data from Coronas-Photon
(Electron-M PESCA)

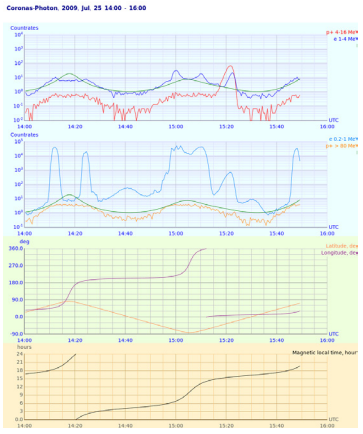

Short-time forecast of killer electrons

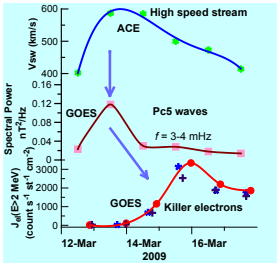

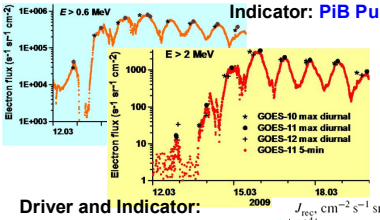

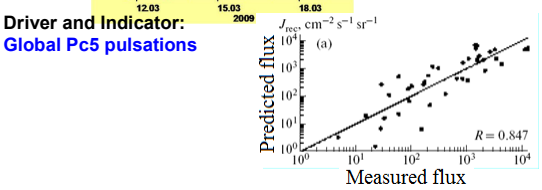

A chain of physical processes leading to the radiation belt electron acceleration up to relativistic energy has been traced. It includes interaction of the solar wind high speed stream with the magnetosphere, generation of global ULF waves, occurrence of medium energy electrons, and their acceleration by ULF waves due to drift resonance mechanism. Basing on this scenario, a method for a short-term prediction of killer electron fluxes was proposed. The method combines information about PiB pulsations as an indicator of medium energy electrons and global Pc5 as a driver for electron acceleration.

Degtyarev, V.I., et al., Adv. Space Res., V. 43 (5), 829–836, 2009.
Potapov, A.S. and Polyushkina T.N., Geomagnetism and Aeronomy, 50(8), 28–34, 2010.

Contact: A.S. Potapov (potapov@iszf.irk.ru)

Complex Active Experiments "Sura – ISS"

For the first time in two complex experiments (from all conducted in 2007-2010) with Sura heating facility similar disturbances in a magnetic field of the Earth which can be interpreted as a signature of substorms, stimulated by heating facility emission are registered. Variations of magnetic field horizontal component observed by Karpogory observatory are shown. Color indicate the periods of the heating facility operation. The presented results prove to be true by measurements on the ISS and DEMETER spacecraft.

Contact Yu. Ruzhin (ruzhin@izmiran.ru)

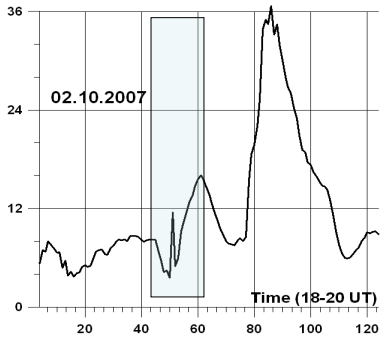

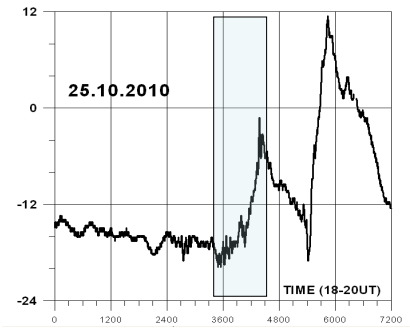

IV. Solar Wind and Interplanetary Magnetic Field

Planned space missions

INTERHELIOPROBE

The mission is aimed at the study of the inner heliosphere and the Sun. After a short ecliptic phase of the mission , the gravity-assisted maneuvers at Venus can be used for inclining the SC orbit to the ecliptic plane and conducting out-of-ecliptic observations of the Sun. The mission scientific payload will comprise the instruments for remote observations of the Sun (X-ray telescope-spectrograph, coronagraph, magnetograph, and photometer) and in-situ measurements in the heliosphere (magnetometer, solar-wind electron analyzer, plasma analyzer, analyzer of solar neutrons, detector of charged particles, gamma-ray spectrometer, X-ray spectrometer, and wave complex).

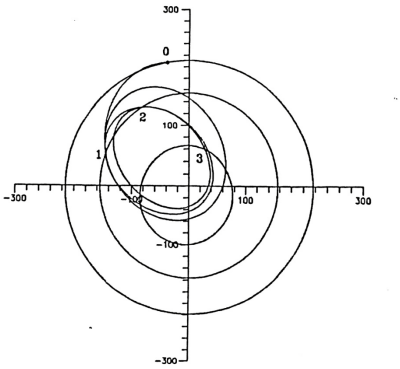

Interhelioprobe ballistic scheme.

Contact V.D.Kuznetsov (kvd@izmiran.ru)

Planned space missions

Polar Ecliptic Patrol

The mission is aimed at the study of the global pattern of solar activity, including its manifestations in the heliosphere and near-Earth space. The mission will comprise two small satellites. By gravity-assisted maneuvers at Venus, the satellites will be placed on heliocentric orbits inclined to the ecliptic plane at an angle to each other at distances about 0.5 AU from the Sun. The satellites on the orbits will be shifted about one another by a quarter of a period (one period is about 130 days). S*imultaneous monitoring* of the near-ecliptic and polar regions planned to be carried.
Stage A started in 2009, will be devoted to developing the details of the ballistic characteristics of the mission, its scientific tasks and instruments, and the tentative outward appearance of the spacecraft.

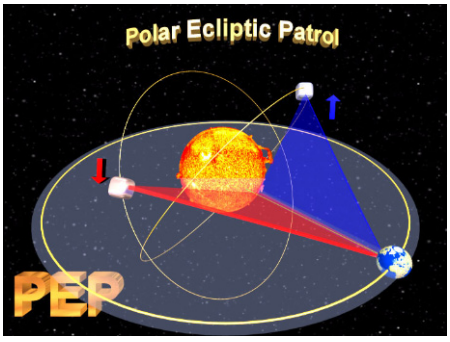

Ballistic scheme of the Polar Ecliptic Patrol.

Contact V.D.Kuznetsov (kvd@izmiran.ru)

Observations of global oscillations of the Sun within the SOKOL experiment on board the CORONAS-FOTON mission

CORONAS-I (1994 - 2001) and CORONAS-F (2001 – 2005) helioseismic observations aimed at the study of global oscillations of the Sun were continued on board the CORONAS-FOTON mission with the SOKOL multi-channel solar photometer designed at IZMIRAN.
The relative amplitude of the oscillation p-modes in the infrared spectral range was determined to be $0.7 \cdot 10^{-6}$ of the total solar irradiance for the 1100 nm channel and $0.5 \cdot 10^{-6}$, for the 1550 nm channel. These values, together with the relative amplitudes of oscillations derived from the CORONAS-F/DIFOS data, were used to plot the oscillation relative amplitude as a function of the observation wavelength.
Calculations by the inverse problem method have revealed that **the global oscillations in the photosphere are composed of the related temperature waves and oscillation p-modes** and that **periodic fluctuations of brightness of the Sun and solar-type stars are due** not to the p-modes (as is usually believed), but rather **to the temperature waves** generated by the latter as a result of nonadiabatic oscillations in the photosphere

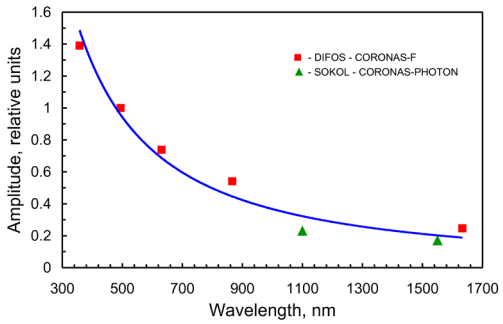

The amplitude of global five-minute oscillations as a function of wavelength. Squares – CORONAS-F/DIFOS data; triangles - CORONAS-PHOTON/SOKOL data.

Contact V.D.Kuznetsov (kvd@izmiran.ru)

Solar Dipole Magnetic Moment

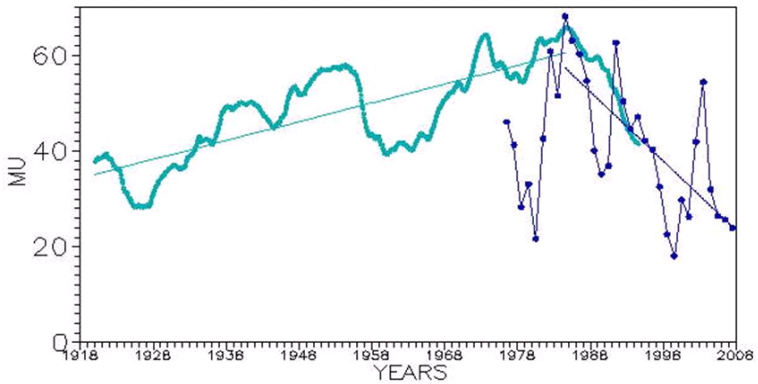

*It was shown (*V. I. Makarov, V. N. Obridko, A. G. Tlatov. *Astronomicheski Zhurnal , Vol. 78,No. 9, 2001; V.I.* Makarov , *A.G.Tlatov, D.K.Callebaut, V.N.Obridko, Solar.Phys., 206, 2002) that magnetic moment of solar dipole was growing up to 1984-1985, but later polar magnetic field strength is shown to have decreased steadily during the last three solar cycles. This is because the increase in the dipole magnetic moment observed from 1915 to 1976 has changed into a decrease in the last three cycles. The set of data considered may be indicative of the possible approach of a sequence of low solar cycles (Obridko and Shefting 2009, Astronomy Letters, 2009, Vol 35, No. 4).*

Contact V. Obridko (obridko@izmiran.ru)

Quasi-periodic fluctuations detected in MARS-EXPRESS coronal radio sounding observations.

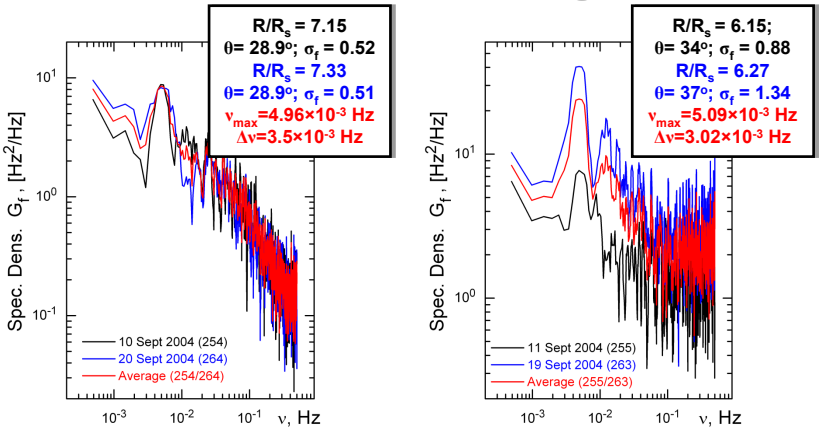

The MARS EXPRESS Coronal-Sounding Experiment has provided observational evidence of quasi-periodic frequency fluctuations of radio signals in the range 5-10 solar radii, implying that MHD (Alfven) waves with periods near 4 minutes ($\nu \approx 4$ mHz) are continuously present in the solar wind acceleration region.
The coronal-sounding observations support the idea that 5-min oscillations play an important role in the dynamics of the solar corona and solar wind.

Contact I.V. Chashey (chashey@prao.ru)

Kinematics of coronal mass ejections and coronal blast waves (ISTP SB RAS, LPI RAS, IZMIRAN, UAPO FEB RAS, Nobeyama observatory)

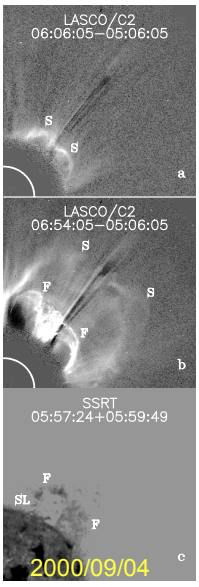

Complementary multi-spectral observations of a few eruptive filaments and CMEs from the low corona up to the outer one were analyzed. It is shown that a self-similar approximation correctly describes the kinematics of

- Coronal blast waves (power-law height-time dependence),
- Coronal mass ejections (presumably up to ~30R$_\odot$).

Methods for estimation of ejected mass ($3 \cdot 10^{15}$ g) from the absorption depth in Hα or EUV lines as well as radio data are developed.

Contact V.V.Grechnev (grechnev@iszf.irk.ru)

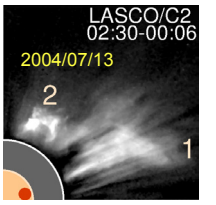

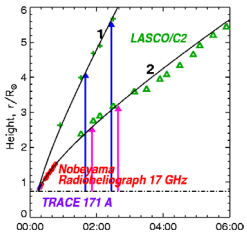

Symbols mark the measured points, and curves present the calculations.
Expansion is self-similar

Oscillations in solar chromospheric grid and coronal heating.

It is found that at the edges of chromospheric super granulation network, predominating oscillations have a period of ~5 min., while inside it - the main period is ~3 min. In the solar corona oscillations with the same periods (p-modes) were also seen in radiowaves at 11 and 37 GHz.
It is shown that the origin of such oscillations in the corona is due to parametric interaction of coronal loops with p-modes. The parametric resonance may work as an effective channel for transfering the energy of photospheric oscillations to the corona. It offers the challenge to understanding the heating mechanism of the solar corona.

Wavelet filtration for 5 min/ mode of line-of-site velocity signal from photosphere and chromosphere at the base of coronal holes.
The line-of-site velocity profiles (right panel) show 40-50 s. velocity delay between photosphere and chromo-sphere corresponding to vertical propagation velocity of 40-45 km/s.

Contact A.V.Stepanov
(stepanov@gao.spb.ru)

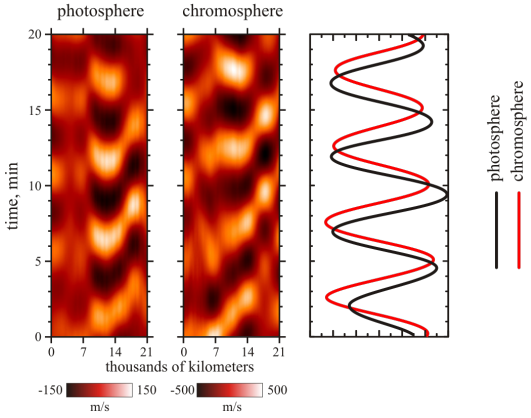

Spiral structure of the magnetic field above coronal holes

The multi-wavelength polarization data of RATAN-600 revealed that above stable active regions magnetic field has a spiral structure. Magnetic flux tube spreads upward as a spiral with width of ~0.4 helio deg. Magnetic fields of about 600 G are determined at heights up to 25 000 km.

Example of magnetic field structure above active region NOAA 0953 on 03-02 May 2007

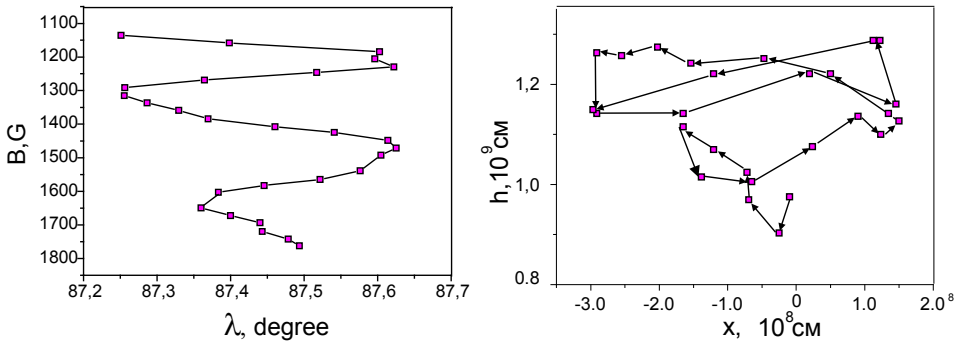

Monotonous polarization spectrum → monotonous B (λ) → altitudinal structure of active region h(x)

Contact V.M. Bogod (vbog_spb@mail.ru)

High correlation is found between the coronal hole contrast and the solar wind velocity

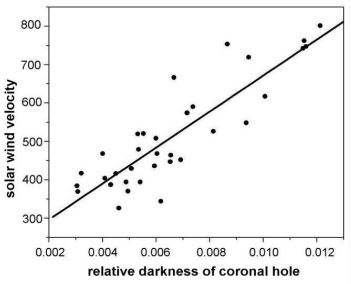

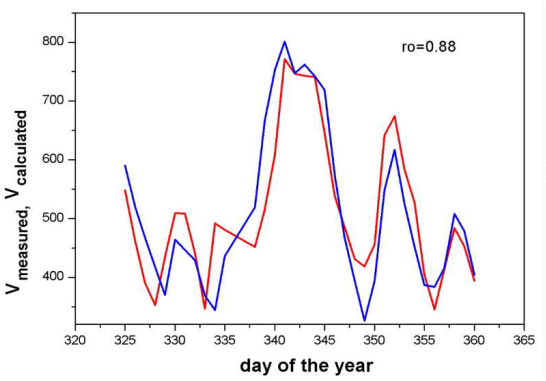

Contact V.N. Obridko
(obridko@izmiran.ru)

A scenario of initiation and development of a flare with filament ejection.

A scenario of initiation and development of a flare with filament ejection has been constructed for flares which are not described by existing two-dimensional models. The model takes into account the effects appearing due to interaction between two rising and untwisting magnetic ropes located at the base of the funnel-shaped magnetic domain with the zero point in its top. Using a three-dimensional model, we managed to explain the dynamics of the flare process manifesting itself in flare emissions in different bands.

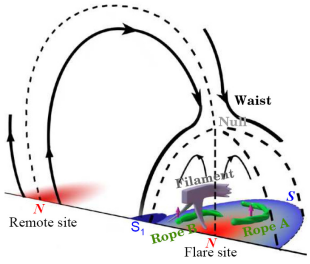

Configuration before the flare.
Dashed lines indicate separatrices.

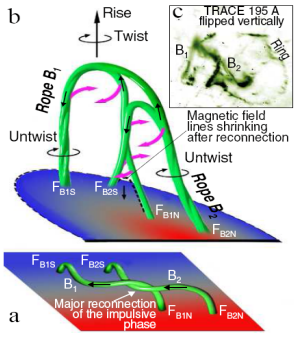

A scheme of the flare development during partial magnetic reconnection of two ropes. Untwisting of ropes B1 and B2 results in twisting of a new large-scale rope that is formed during the partial magnetic reconnection. Black arrows on the bundles indicate directions of current flow.
a)initial position of ropes;
b)situation after the impulsive phase;
c)image of the flare in the 195Å emission (TRACE).

Contact A.T.Altyntsev(altyntsev@iszf.irk.ru)

Unified statistical distributions of solar X-ray flare durations.

The vast data base containing about 40000 X-ray solar flare events compiled and visualized as histograms and movies is collected on the site (http://dec1.sinp.msu.ru/~pavrus/) for different flare classes according to their intensities. Spacecraft measurements were analyzed during 21nd-23rd solar cycles with a time resolution of 1 min. It is found that the rising time and total duration distributions follow the lognormal laws with parameters depending on the flare class and the solar cycle. One-modal distributions cover both 'impulsive' flares (~20-30 min duration) and 'long-duration' events (> 30 min and up to many hours) at the level of 1-3 sigma.

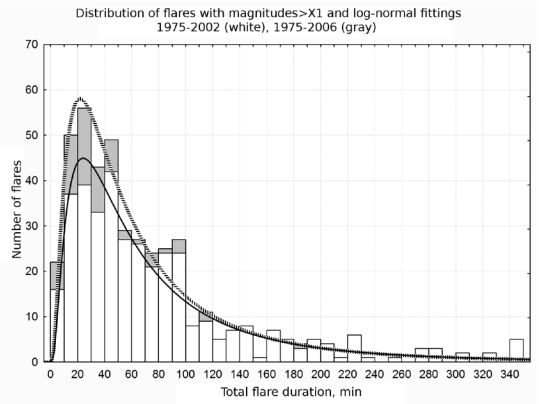

Figure shows the number of flares (ordinate) versus their total duration (min, abscissa) for the X-ray flares of the X1 class and higher, during 1975-2002 and 1975-2006 together with their lognormal approximations. Excesses and fluctuations of histograms are shown in gray.

Contact I.S. Veselovsky
(veselov@dec1.sinp.msu.ru)

Study of the reasons of extreme disturbances on the Sun and in the heliosphere in 23d solar activity cycle (SINP MSU, IKI RAS, IZMIRAN)

Thorough experimental and theoretical analyses of different scale phenomena were done. It is found that the strongest CMEs have angular dimensions of more than 180 deg. and include a number of active regions.

In MHD and kinetic approaches the dimensionless Trieste numbers were used to describe an opening degree of loop structures for mass flux, momentum and energy. Features of loops are critical for the development of extreme disturbances.

Flare-like and CME-like events differ by another dimensionless parameter characterizing a relevant role of electromagnetic losses and kinetic energy of plasma motion in eruptive process.

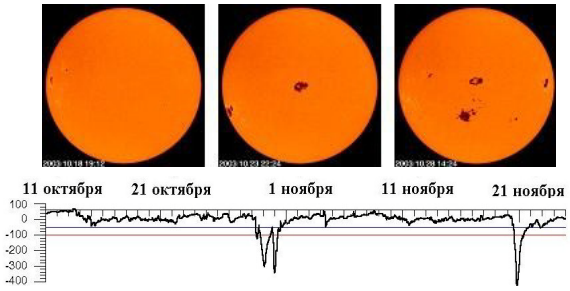

The motion of active regions with rotation of the Sun (from left to right) as seen by SOHO, and Dst-index.

Contact I.S.Veselovsky (veselov@dec1.sinp.msu.ru)

Study of fine spectral features of polarized emission at pre-flare stage of active regions.

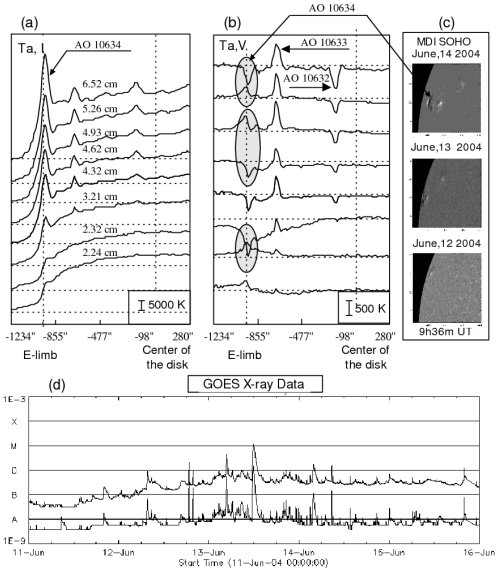

On the basis of multi-wavelength observations made with the one-dimensional RATAN-600 radio telescope, we study the inversion of the circular polarization in the solar microwave emission at different frequencies.

The inversion is detected in the emission of flare-producing active regions (FPAR) at various stages of their development, starting from the pre-flare stage.

On the Figure:

a)Intensity scans of the Sun at different wavelengths,
b)Polarization scans with polarization inversions (ovals)
c)Appearance ofthe active region on the disk
d)Flare activity of AR according GOES-satellite

Contact V.M.Bogod (vbog@sao.ru)

V.Observatories, Instruments, Surveys, and Analysis

1. During past four years the E.K.Fedorov Institute of Applied Geophysics has been performing within the framework of the National Heliogeophysical Service and Regional Warning Center (RWC) Russia of the International Space Environment Service (ISES) the following works-
-conducted heliogeophysical observations using its own ground-based and space facilities,
-coordinated works of other observatories in the Russian region incorporated into the observational network of the Service (I0 ionospheric and 13 magnetic stations).
-collected and analyzed data from the network, prepared and issued current summaries and forecasts, performed an operative exchange of the information with other RWCs.

Development of ground-based observations (IZMIRAN)

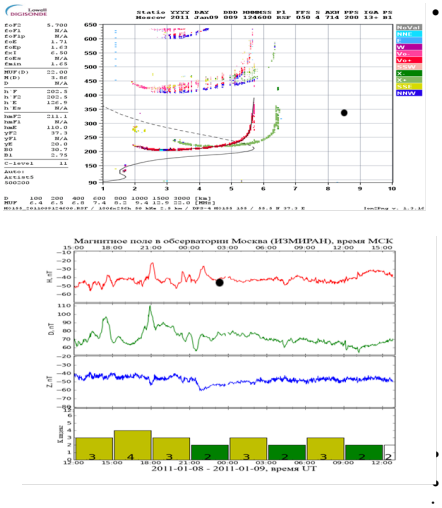

The development and improvement of ground-based geophysical measurement network was continued. In particular, it was put into regular operation the new DPS-4 ionosonde, capable to measure the angles of arrival of radio waves reflected from the ionosphere, to assess their angular spectrum and measure the motion of ionospheric irregularities in addition to the standard ionograms. Ionosonde data are available on the Internet in real time. Six sets of quartz digital magnetometers were manufactured in 2010, some of which are already installed on the existing magnetic observatories to get digital 1 sec magnetic data. Others will be installed in the next year.

Contact :http://sphere.izmiran.ru:43080
http://serv.izmiran.ru

Modernization of the Siberian Solar Radio Telescope (SSRT)

The 10-antenna prototype of multiwave radioheliograph was developed in the course of modernization of the Siberian Solar Radio Telescope (SSRT). The frequency band is 4-8 GHz. The testing results showed that the used technologies provided the planned parameters of the radioheliograph.

Antennas of the prototype as part of SSRT

Contact A.T. Altyntsev
altyntsev@iszf.irk.ru

Results obtained from ground-based observations.

Data are mainly collected by:

- Central Astronomical Observatory of Russian Academy of Sciences at Pulkovo (CAO RAN, http://www.gao.spb.ru):
  - Kislovodsk Solar Mountain Station
  - Pulkovo Horizontal solar telescope
  - The Big Pulkovo radio telescope
- The Special Astrophysical Observatory of Russian Academy of Sciences (Nizhny Arhyz, http://www.sao.ru/):
  - RATAN 600
- Institute of Solar-Terrestrial Physics of Russian Academy of Sciences, Siberian Branch (ISTP RAS, http://iszf.irk.ru/)
  - Sayan Solar observatory
  - Siberian solar radio telescope
  - Baikal astrophysical observatory
- Radiophysical research institute (NIRFI, http://solar.nirfi.sci-nnov.ru/RAS_Zimenki/)
  - Zimenki Radio Astronomical Station

Data bases of synoptic solar observations

As a result of 60 years lasted solar synoptic observations by Kislovodsk Solar Mountain Station of the Pulkovo observatory, a set of different data bases parameterizing a long-term behavior of solar activity were created.

Optimal astroclimate in Kislovodsk provides regular and permanent solar observations. Kislovodsk observational series of the classical indices (i.e. Zurich relative sunspot number and Greenwich sunspot area) are probably preferable to extend world synoptic observations since the 1980s till nowadays.

Data Bases:

- Electronic archive of synoptic observations by Kislovodsk Mountain Station http://www.solarstation.ru/?lang=ru&id=archivedata/
- The electronic bulletin «*Solnechniye Danniye*» http://www.gao.spb.ru/russian.win/sd/
- The Interactive database on solar activity in a system of "Pulkovo catalogue of solar activity" http://www.gao.spb.ru/database/csa/

and others.

Contact Yu. A. Nagovitsin (nag@gao.spb.ru)

Center for analysis of multiwave solar observations by RATAN-600.

http://www.spbf.sao.ru/

The center is created on the basis of St.-Petersburg branch of the Special Astrophysical Observatory of RAS.

Continuous solar observations by the RATAN-600 radiotelescope in the 3 - 18 GHz range with 1 % frequency resolution are automatically collected and processed. The information is presented through the convenient web-based interface for analysis, modeling, and comparison with other ground-based and space observations, such as Siberian Solar Radio Telescope (SSRT, Russia), Nobeyama Radioheliograph (Japan), SOHO mission and others.

Contact S.Tokhchukova (susan@sao.ru)

Example of Solar Activity analysis

http://www.spbf.sao.ru/prognoz/index.htm

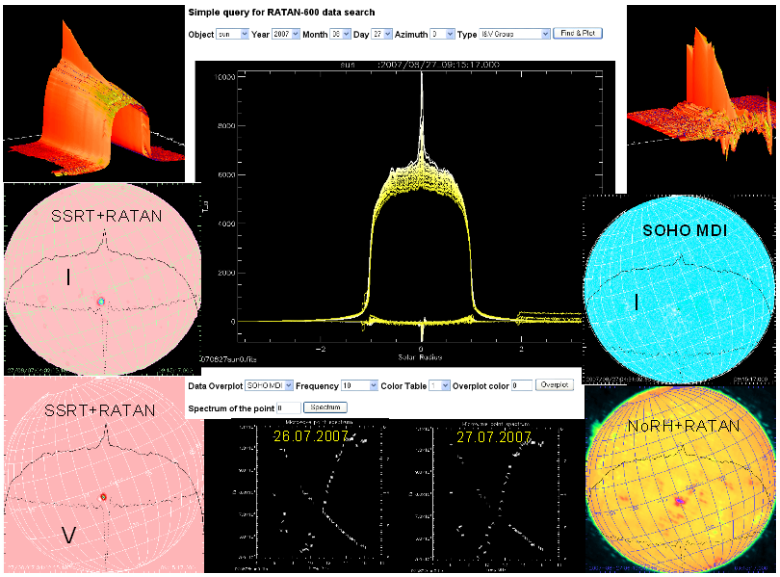

Explanation of the previous slide

Web site http://www.spbf.sao.ru/prognoz/ is for presentation of multiwave solar observations from RATAN-600 radiotelescope.

In the center: the multiwavelength scan in intensity and circular polarization.

Below: the calculated spectra of active region, which located in the center of the disk for two consequent days.

On the left : 3-D presentation of multiwavelength intensity of RATAN-600 scan (top),
Comparison with radioheliograph SSRT intensity map (middle),
Comparison with SSRT polarization map (bottom).

On the right: 3-D presentations of multiwave polarization of RATAN-600 scan (top),
Comparison with satellite SOHO MDI map (middle),
Comparison with radioheliograph Nobeyama Intensity map (botom),

Reconstruction of Space Weather features on long time scales. (GAO RAS, PhTI RAS, ISTP SB RAS)

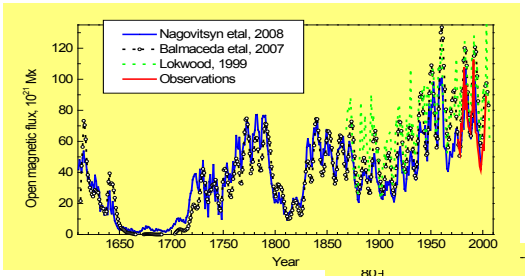

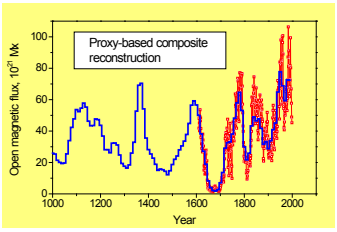

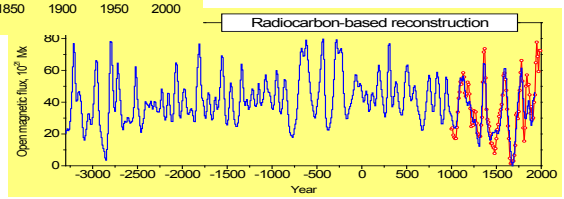

Modern mathematical methods and different types of experimental data were used for reconstruction of main physical parameters describing the Space Weather in the past on time scales from 10^2 to 10^4 years.

Contact Yu. A. Nagovitsin (nag@gao.spb.ru)

A forecast of solar activity variation in the 24th solar cycle.

A forecast of mean and maximum numbers of sunspot groups over the upcoming 24th solar cycle, was made using paleoastrophysical information about the solar activity throughout the last 10000 years. It was shown that from the point of view of solar paleoastrophysics the current cycle should be moderate – the maximum number of sunspot groups might reach 68-101, and the cycle average value – 34-51. Probability of a high maximum sunspot number (more than 160) predicted by some authors, was found to be weak – less than 2 %.

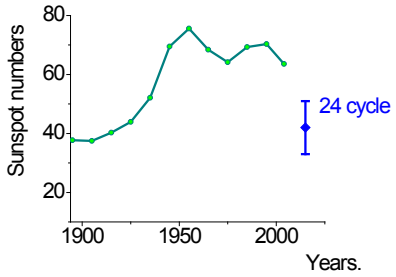

Sunspot number over the last 100 years and paleoastrophysical forecast for the current 24-th cycle.

Contact V.A. Dergachev (v.dergachev@mail.ioffe.ru)

North–South Asymmetry in Sunspot Formation, Mean Sunspot Latitudes, and the Butterfly Diagram during Maunder minimum

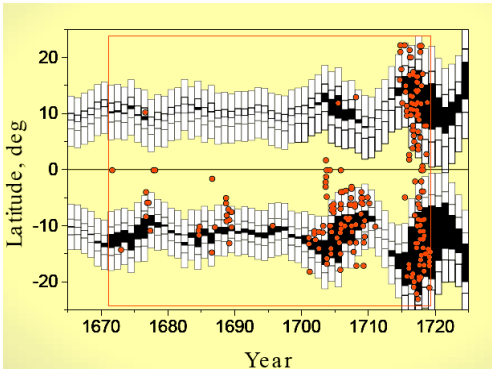

Model butterfly diagram in the Maunder minimum of solar activity (dark areas) and a comparison with the observations by Picard and de la Hire of 1671–1718 (orange circles). The vertical rectangles show 1σ and 3σ confidence intervals for the model in latitude.

DPS (Decomposition in pseudo-Phase Space) approach (*Nagovitsyn et al, Solar Phys.* ***224****, 2004*) to reconstructing solar activity in the past is used to study its space-time evolution. It is shown that we can now reconstruct not only the general level of solar activity on long timescales, but also particular aspects of its development: sunspot dominance in either hemisphere, the drift and latitude spread of the sunspot-formation zone, and features in the spatial distribution of the activity at specific epochs, such as the Maunder minimum.

Contact Yu.A. Nagovitsyn
(nag@gao.spb.ru)